

Magnetic-Field-Driven Localization of Light in a Cold-Atom Gas

S. E. Skipetrov^{1,2,*} and I. M. Sokolov^{3,†}

¹*Université Grenoble Alpes, LPMMC, F-38000 Grenoble, France*

²*CNRS, LPMMC, F-38000 Grenoble, France*

³*Department of Theoretical Physics, St. Petersburg State Polytechnic University, 195251 St. Petersburg, Russia*

(Received 13 October 2014; published 5 February 2015)

We discover a transition from extended to localized quasimodes for light in a gas of immobile two-level atoms in a magnetic field. The transition takes place either upon increasing the number density of atoms in a strong field or upon increasing the field at a high enough density. It has many characteristic features of a disorder-driven (Anderson) transition but is strongly influenced by near-field interactions between atoms and the anisotropy of the atomic medium induced by the magnetic field.

DOI: 10.1103/PhysRevLett.114.053902

PACS numbers: 42.25.Dd, 05.60.Gg, 32.80.Qk, 42.50.Nn

The transition from extended to localized eigenstates upon increasing disorder in a quantum or wave system is named after Philip Anderson who was the first to predict it for electrons in disordered solids [1]. More recently, this transition was studied for various types of quantum particles (cold atoms [2], Bose-Einstein condensates [3]) as well as for classical waves (light [4–6], ultrasound [7,8]). In the most common case of time-reversal symmetric systems invariant under spin rotation Anderson transition takes place for a three-dimensional (3D) disorder only, eigenstates of low-dimensional systems being always localized [9,10]. Anderson localization of light may find applications in the design of future quantum-information devices [11], miniature lasers [12], and solar cells [13]. However, no undisputable experimental observation of optical Anderson transition in 3D exists to date since alternative explanations were proposed for all published reports of it [14–16]. Moreover, we have recently shown that the simplest theoretical model in which light is scattered by point scatterers (atoms) does not predict Anderson localization of light at all [17].

In the present Letter, we show that an external magnetic field may induce a transition between extended and localized states for light in a gas of cold atoms. Magnetic field is an important and unique means of controlling wave propagation in disordered media. On the one hand, it breaks down the time-reversal invariance leading to a suppression of weak localization in electronic [18] and optical [19] systems and to metal-insulator transitions in topological insulators [20]. On the other hand, by profoundly modifying the scattering properties of individual scatterers the magnetic field can produce an enhancement of the coherent backscattering peak for light scattered by atoms with a degenerate ground state [21,22]. Our work adds a new element in the mosaic of magnetic-field-induced phenomena in disordered systems by demonstrating that the removal of degeneracy of the excited atomic state due to the Zeeman effect and the resulting

reduction of the strength of resonant dipole-dipole interactions between nearby atoms [23] are sufficient to induce a transition from extended to localized states in a dense atomic system where Anderson localization does not take place in the absence of the field [17]. This critical phenomenon stands out from other magneto-optical effects that take place in disordered media (including also the photonic Hall effect [24] and Hanle effect in coherent backscattering [25]) which only give rise to weak corrections to wave transport.

We consider an ensemble of $N \gg 1$ identical two-level atoms at random position $\{\mathbf{r}_i\}$ inside a spherical volume V of radius R . The resonant frequency ω_0 of atoms defines the natural length scale $1/k_0 = c/\omega_0$, where c is the vacuum speed of light. The ground state $|g_i\rangle$ of an isolated atom i is nondegenerate with the total angular momentum $J_g = 0$, whereas the excited states $|e_i\rangle$ is threefold degenerate with $J_e = 1$. The three degenerate substates $|e_{im}\rangle$ correspond to the three possible projections $m = 0, \pm 1$ of the total angular momentum \mathbf{J}_e on the quantization axis z . The natural lifetime $1/\Gamma_0$ of the excited state sets the time scale of the problem. The atoms are subject to a uniform magnetic field $\mathbf{B} \parallel z$ and interact with the free electromagnetic field surrounding them. The system “atoms + field” is described by the following Hamiltonian [22,26,27]:

$$\begin{aligned} \hat{H} = & \sum_{i=1}^N \sum_{m=-1}^1 \hbar \omega_0 |e_{im}\rangle \langle e_{im}| + \sum_{\mathbf{s} \perp \mathbf{k}} \hbar c \mathbf{k} \left(\hat{a}_{\mathbf{k}\mathbf{s}}^\dagger \hat{a}_{\mathbf{k}\mathbf{s}} + \frac{1}{2} \right) \\ & - \sum_{i=1}^N \hat{\mathbf{D}}_i \cdot \hat{\mathbf{E}}(\mathbf{r}_i) + \frac{1}{2\epsilon_0} \sum_{i \neq j}^N \hat{\mathbf{D}}_i \cdot \hat{\mathbf{D}}_j \delta(\mathbf{r}_i - \mathbf{r}_j) \\ & + g_e \mu_B \mathbf{B} \cdot \mathbf{J}_e. \end{aligned} \quad (1)$$

Here \hbar is the Planck’s constant divided by 2π , \mathbf{k} and \mathbf{s} are the wave and the polarization vectors of the modes of the free electromagnetic field, $\hat{a}_{\mathbf{k}\mathbf{s}}^\dagger$ ($\hat{a}_{\mathbf{k}\mathbf{s}}$) are the corresponding creation (annihilation) operators, $\hat{\mathbf{D}}_i$ are the atomic dipole

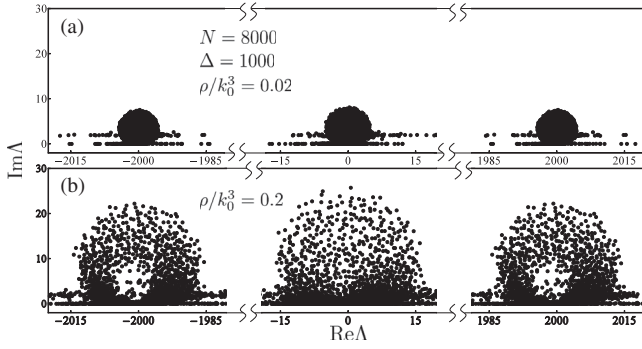


FIG. 1. Complex eigenvalues Λ of a representative random realization of the Green's matrix for $N = 8 \times 10^3$ two-level atoms in a strong magnetic field ($\Delta = 10^3$) at low (a) and high (b) densities of atoms.

operators, $\hat{\mathbf{E}}(\mathbf{r}_i)$ is the electric displacement vector divided by the vacuum permittivity ϵ_0 , μ_B is the Bohr magneton, and g_e is the Landé factor of the excited state.

Previous work [28,29] demonstrated that in the absence of magnetic field ($\mathbf{B} = 0$), the degrees of freedom corresponding to the electromagnetic field can be traced out leading to an effective Hamiltonian describing the

dynamics of N atoms coupled by the electromagnetic field. This effective Hamiltonian takes the form of a $3N \times 3N$ Green's matrix G describing the propagation of light between the atoms [17]. The same approach can be used when $\mathbf{B} \neq 0$ leading to the following Green's matrix:

$$G_{e_{im}e_{jm'}} = (i - 2m\Delta)\delta_{e_{im}e_{jm'}} - \frac{2}{\hbar\Gamma_0}(1 - \delta_{e_{im}e_{jm'}}) \times \sum_{\mu,\nu} d_{e_{im}g_i}^\mu d_{g_j e_{jm'}}^\nu \frac{e^{ik_0 r_{ij}}}{r_{ij}^3} \times \left\{ \delta_{\mu\nu} [1 - ik_0 r_{ij} - (k_0 r_{ij})^2] - \frac{r_{ij}^\mu r_{ij}^\nu}{r_{ij}^2} [3 - 3ik_0 r_{ij} - (k_0 r_{ij})^2] \right\}, \quad (2)$$

where $\Delta = g_e \mu_B B / \hbar \Gamma_0$ is the Zeeman shift in units of the natural line width, $\mathbf{d}_{e_{im}g_i} = \langle J_e m | \hat{\mathbf{D}}_i | J_g 0 \rangle$, and $\mathbf{r}_{ij} = \mathbf{r}_i - \mathbf{r}_j$.

In the absence of magnetic field ($\mathbf{B} = 0$) the eigenvalues of the Green's matrix G concentrate in a roughly circular domain on the complex plane roughly symmetric with respect to the vertical axis $\text{Re}\Lambda = 0$ and almost touching

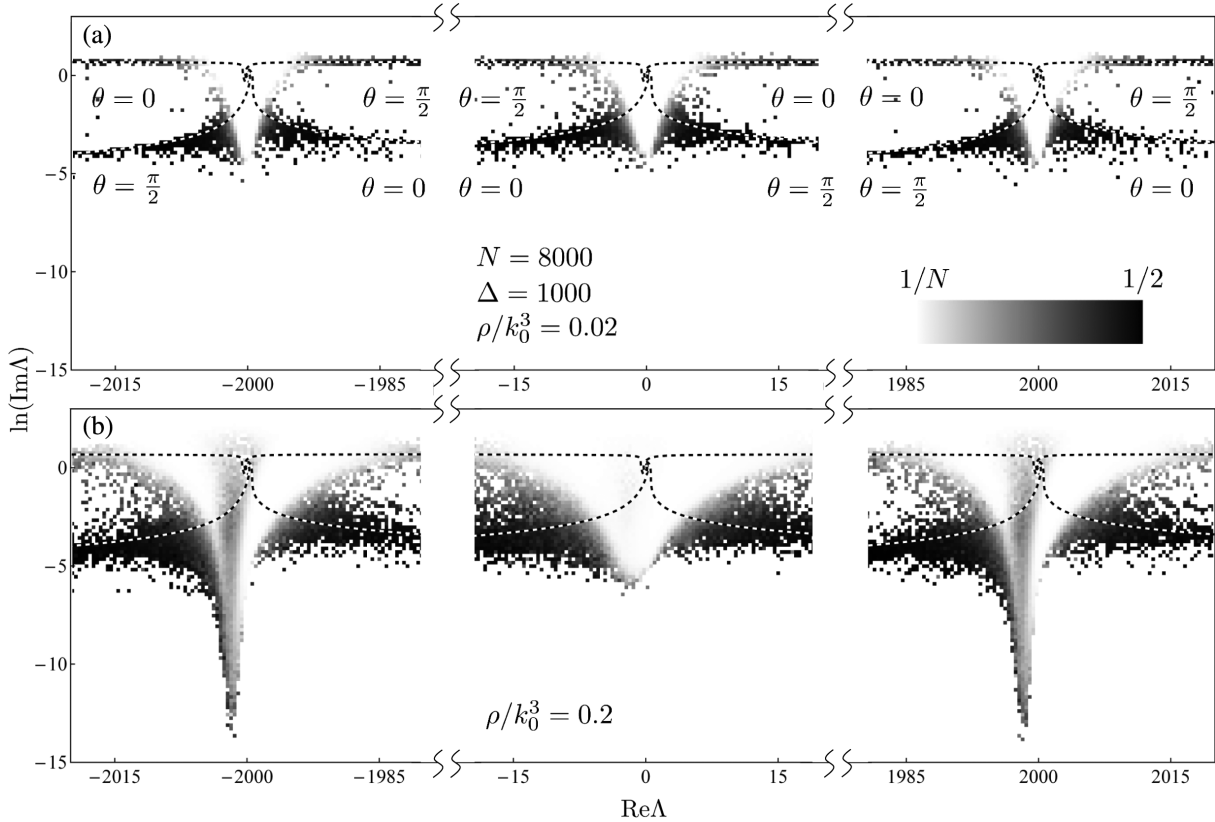


FIG. 2. Gray-scale maps of the average IPR at low (a) and high (b) densities of atoms in a strong magnetic field $\Delta = 10^3$. Dashed lines show lines along which the eigenvalues of a two-atom system would be situated for atoms placed along the direction of magnetic field ($\theta = 0$) or perpendicular to it ($\theta = \pi/2$). For $0 < \theta < \pi/2$ the corresponding eigenvalues are in between the two lines. The gray level of each small square in the figure is obtained by averaging over IPR of all eigenvalues that fall inside the square for 16 different realizations of the random Green's matrix.

the horizontal axis $\text{Im}\Lambda = 0$ [17,30]. The field splits the eigenvalues into three equal groups centered around $\text{Re}\Lambda = -2m\Delta$ ($m = 0, \pm 1$) [31], see Fig. 1. The three groups of eigenvalues become well separated in the limit of strong magnetic field $\Delta \gg 1$ to which we will restrict our consideration in the present Letter. Although at a low density $\rho = N/V$ the three groups of eigenvalues are similar [Fig. 1(a)], the groups corresponding to $m = \pm 1$ start to differ significantly from the $m = 0$ group at higher densities [Fig. 1(b)]. In particular, the $m = \pm 1$ groups of eigenvalues develop “holes” that were previously associated with Anderson localization in the framework of the scalar model of wave scattering [32,33].

To see whether localized states indeed appear at high densities of atoms, we analyze the inverse participation ratios (IPRs) of eigenvectors ψ_n of the Green’s matrix G , $\text{IPR}_n = \sum_{i=1}^N |\psi_{ne_i}|^4 / (\sum_{i=1}^N |\psi_{ne_i}|^2)^2$, where $|\psi_{ne_i}|^2 = \sum_{m=-1}^1 |(\psi_{ne_i})_m|^2$ is the square of the length of the vector $\psi_{ne_i} = \{(\psi_{ne_i})_m\}$. Low $\text{IPR} \sim 1/N$ corresponds to an extended state whereas $\text{IPR} \sim 1/M > 1/N$ signals a state localized on $M < N$ atoms. Figure 2(a) shows that at low density of atoms most of the eigenvectors have low IPRs with the eigenvectors localized on pairs of closely located atoms being an exception. These “subradiant” states exist at any density and should be distinguished from localized states that are due to the multiple scattering of light on many atoms and that appear at higher densities in relatively narrow bands of frequencies $\text{Re}\Lambda$ on the left from the resonances $\text{Re}\Lambda = \pm 2\Delta$ [see Fig. 2(b)]. These states may have smaller IPRs than the subradiant states but they have significantly longer lifetimes (i.e., smaller $\text{Im}\Lambda$).

The appearance of states localized on large clusters of atoms in a magnetic field is due to the removal of degeneracy of the excited states $|e_i\rangle$ by the field. As a result, the transitions $|g_i\rangle \rightarrow |e_{im}\rangle$ effectively decouple for different m since photons scattered on these transitions

have frequencies discrepant by $\approx 2g_e\mu_B B/\hbar \gg \Gamma_0$. As a consequence, a behavior similar to the scalar case may be expected for a given m with, in particular, localized states appearing at high densities of atoms as found in the scalar model [17]. However, as follows from Fig. 2, this naive picture is largely oversimplified because it does not explain the absence of localized states near $\text{Re}\Lambda = 0$ corresponding to $m = 0$. A more detailed study shows that indeed, the full vector problem can be reduced to an effective scalar one in the limit of strong magnetic field, but the effective Green’s matrix following from this analysis is different from the one corresponding to scalar waves. We have found that for $\Delta \gg 1$, the group of eigenvalues corresponding to a given m can be approximately found by diagonalizing the effective $N \times N$ Green’s matrix

$$G_{ij} = (i - 2m\Delta)\delta_{ij} + (1 - \delta_{ij}) \frac{e^{ik_0 r_{ij}}}{k_0 r_{ij}} \times \left\{ c_m [1 - (-1)^m \cos^2 \theta] + c_m (-1)^m \left[\frac{i}{k_0 r_{ij}} - \frac{1}{(k_0 r_{ij})^2} \right] (1 - 3\cos^2 \theta) \right\}, \quad (3)$$

where $c_m = (3/8)[3 + (-1)^m]$ and θ is the angle between \mathbf{r}_{ij} and the z axis.

Equation (3) explains the differences between $m = 0$ and $m = \pm 1$ seen in Figs. 1 and 2. First, the far-field contribution to G_{ij} given by the second line of Eq. (3) varies from 0 to 1 for $m = 0$ and from $\frac{1}{2}$ to 1 for $m = \pm 1$ as a function of θ . It is thus closer to its scalar-wave value of 1 in the former case, suggesting that the case of $m = \pm 1$ may be better approximated by the scalar model than the case of $m = 0$. Second, the near-field term [the third line of Eq. (3)] is a factor of 2 smaller for $m = \pm 1$ than for $m = 0$. Because near-field terms responsible for resonant dipole-dipole

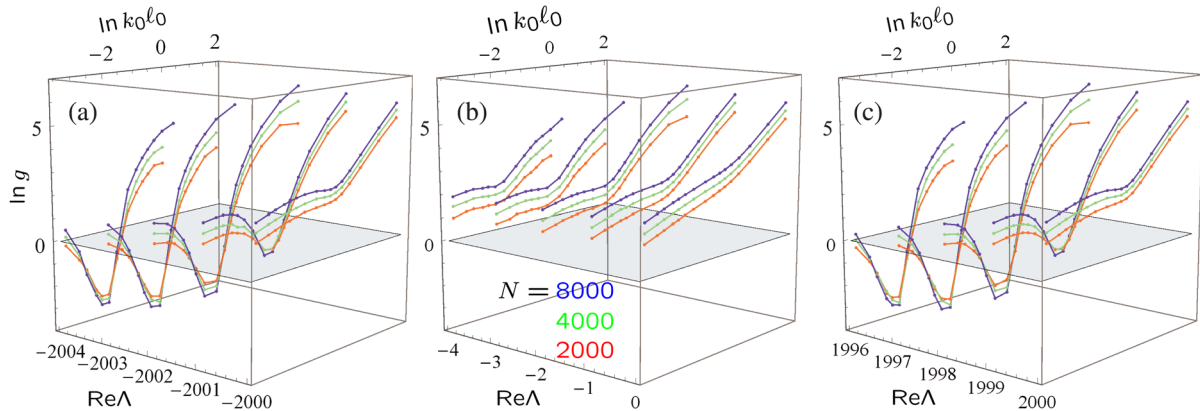


FIG. 3 (color online). Thouless number g as a function of the bare Ioffe-Regel parameter $k_0 \ell_0 = k_0^3 / 6\pi\rho$ for a strong magnetic field $\Delta = 10^3$. The curves are obtained by averaging over a unit interval of $\text{Re}\Lambda$ around their positions and over 50, 25, or 16 realizations of random positions of N atoms for $N = 2000, 4000$, and 8000 , respectively. Different curves at the same value of $\text{Re}\Lambda$ correspond to different numbers of atoms N . The gray plane corresponds to $g = 1$.

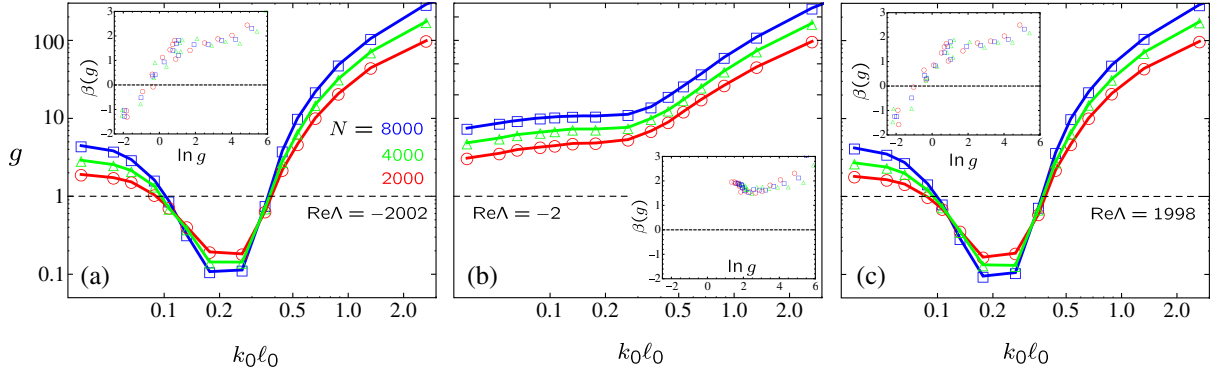


FIG. 4 (color online). Same as Fig. 3 but for selected values of $\text{Re}\Lambda = -2002$ (a), -2 (b), and 1998 (c). The insets show the scaling function $\beta(g)$ estimated from the numerical data of the main plots.

interactions between nearby atoms suppress light scattering [34,35] and prevent Anderson localization [17], their weakness for $m = \pm 1$ is an advantage. We see therefore that both far- and near-field features of Eq. (3) are closer to its scalar approximation for $m = \pm 1$ than for $m = 0$. This explains the appearance of localized states for $m = \pm 1$ rather than for $m = 0$ transitions.

To have a quantitative characterization of the localization transition demonstrated in Fig. 2, we compute the Thouless number $g = \delta\omega/\Delta\omega$ that we define as a ratio of the inverse of the average lifetime of eigenstates $\delta\omega = \langle 1/\text{Im}\Lambda \rangle^{-1}$ to the average eigenvalue spacing along the horizontal axis $\Delta\omega = \langle \text{Re}\Lambda_n - \text{Re}\Lambda_{n-1} \rangle$ [9,17,36]. At a given $\text{Re}\Lambda$, g reaches small values $g < 1$ expected for localized states only at large densities corresponding to $k_0\ell_0 = k_0^3/6\pi\rho < 1$ and only for $\text{Re}\Lambda$ corresponding to $m = \pm 1$ (see Fig. 3), in agreement with Fig. 2. The independence of g from the sample size at the points where curves corresponding to the same value of $\text{Re}\Lambda$ but different N cross—a hallmark of critical behavior—is further illustrated in Fig. 4 where we reproduce $g(k_0\ell_0)$ for $\text{Re}\Lambda$ slightly shifted to the left of the single-atom resonances $\text{Re}\Lambda = -2m\Delta$. The localization transition is also evidenced by the scaling function $\beta(g) = \partial \ln g / \partial \ln k_0 R$ [9] shown in the insets of Fig. 4. $\beta(g)$ changes sign for $\text{Re}\Lambda = -2002$ and 1998 but not for $\text{Re}\Lambda = -2$ proving that the localization transition takes place at large frequency shifts $\text{Re}\Lambda \approx \pm 2\Delta$ but not around the fundamental resonance $\text{Re}\Lambda = 0$.

The localization transition reported here takes place under conditions when not only the disorder-induced multiple scattering of photons is strong but cooperative effects leading to Dicke super- and subradiance [37] and resonant dipole-dipole interactions between neighboring atoms [34,35] are important as well. Therefore, despite its overall similarity with the Anderson transition (see also Ref. [38]), it remains to be seen if this transition can be classified as such. Nonetheless, for light of a given frequency $\omega = \omega_0 - (\Gamma_0/2)\text{Re}\Lambda$ the localized regime $g \lesssim 1$ is realized only in the intermediate range of $k_0\ell_0$ (e.g., $k_0\ell_0 \approx 0.1$ – 0.4 for $\text{Re}\Lambda = -2002$ in Fig. 4) which

corresponds to large sizes of the atomic cloud $k_0 R > 1$ (e.g., $k_0 R \approx 15$ – 24 at $N = 8000$). Hence, the localized states disappear in the Dicke limit $k_0 R < 1$ when the cooperative effects dominate. This suggests that the latter are not the main driving force behind the reported localization transition.

In conclusion, we have found that the magnetic field can induce a transition from extended to localized states for light in an ensemble of identical immobile two-level atoms. This is due to the removal of degeneracy of the excited atomic state by the field and the resulting partial suppression of resonant dipole-dipole interactions between nearby atoms. Our theoretical predictions can be directly verified in experiments with, e.g., Sr atoms that have a non-degenerate ground state and were already used to study multiple scattering of light [46]. Theoretical analysis of light scattering in dense clouds of alkali atoms (such as, e.g., Rb⁸⁵) is, however, much more involved [35,47] and our results cannot be trivially extended to this case.

S. E. S. thanks the Agence Nationale de la Recherche for financial support under Grant No. ANR-14-CE26-0032 LOVE. I. M. S. appreciates financial support from the Russian Foundation for Basic Research (Grant No. RFBR-15-02-01013).

*Sergey.Skipetrov@lpmmc.cnrs.fr

†ims@is12093.spb.edu

- [1] P. W. Anderson, *Phys. Rev.* **109**, 1492 (1958).
- [2] J. Chabé, G. Lemarié, B. Grémaud, D. Delande, P. Szriftgiser, and J.-C. Garreau, *Phys. Rev. Lett.* **101**, 255702 (2008).
- [3] F. Jendrzejewski, A. Bernard, K. Muller, P. Cheinet, V. Josse, M. Piraud, L. Pezze, L. Sanchez-Palencia, A. Aspect, and P. Bouyer, *Nat. Phys.* **8**, 398 (2012).
- [4] D. S. Wiersma, P. Bartolini, A. Lagendijk, and R. Righini, *Nature (London)* **390**, 671 (1997).
- [5] M. Störzer, P. Gross, C. M. Aegerter, and G. Maret, *Phys. Rev. Lett.* **96**, 063904 (2006).

- [6] T. Sperling, W. Bührer, C. M. Aegerter, and G. Maret, *Nat. Photonics* **7**, 48 (2013).
- [7] H. Hu, A. Strybulevych, J. H. Page, S. E. Skipetrov, and B. A. van Tiggelen, *Nat. Phys.* **4**, 945 (2008).
- [8] A. Aubry, L. A. Cobus, S. E. Skipetrov, B. A. van Tiggelen, A. Derode, and J. H. Page, *Phys. Rev. Lett.* **112**, 043903 (2014).
- [9] E. Abrahams, P. W. Anderson, D. C. Licciardello, and T. V. Ramakrishnan, *Phys. Rev. Lett.* **42**, 673 (1979).
- [10] F. Evers and A. D. Mirlin, *Rev. Mod. Phys.* **80**, 1355 (2008).
- [11] L. Sapienza, H. Thyrestrup, S. Stobbe, P. D. Garcia, S. Smolka, and P. Lodahl, *Science* **327**, 1352 (2010).
- [12] J. Liu, P. D. Garcia, S. Ek, N. Gregersen, T. Suhr, M. Schubert, J. Mork, S. Stobbe, and P. Lodahl, *Nat. Nanotechnol.* **9**, 285 (2014).
- [13] F. Pratesi, M. Burrelli, F. Riboli, K. Vynck, and D. S. Wiersma, *Opt. Express* **21**, A460 (2013).
- [14] F. Scheffold, R. Lenke, R. Tweert, and G. Maret, *Nature (London)* **398**, 206 (1999).
- [15] T. van der Beek, P. Barthelemy, P. M. Johnson, D. S. Wiersma, and A. Lagendijk, *Phys. Rev. B* **85**, 115401 (2012).
- [16] F. Scheffold and D. Wiersma, *Nat. Photonics* **7**, 934 (2013).
- [17] S. E. Skipetrov and I. M. Sokolov, *Phys. Rev. Lett.* **112**, 023905 (2014).
- [18] G. Bergmann, *Phys. Rep.* **107**, 1 (1984).
- [19] R. Lenke and G. Maret, *Eur. Phys. J. B* **17**, 171 (2000).
- [20] P. Delplace, J. Li, and M. Büttiker, *Phys. Rev. Lett.* **109**, 246803 (2012).
- [21] O. Sigwarth, G. Labeyrie, T. Jonckheere, D. Delande, R. Kaiser, and C. Miniatura, *Phys. Rev. Lett.* **93**, 143906 (2004).
- [22] O. Sigwarth, G. Labeyrie, D. Delande, and Ch. Miniatura, *Phys. Rev. A* **88**, 033827 (2013).
- [23] K. Afrousheh, P. Bohlouli-Zanjani, J. D. Carter, A. Mugford, and J. D. D. Martin, *Phys. Rev. A* **73**, 063403 (2006).
- [24] G. L. J. A. Rikken and B. A. van Tiggelen, *Nature (London)* **381**, 54 (1996).
- [25] G. Labeyrie, C. Miniatura, C. A. Müller, O. Sigwarth, D. Delande, and R. Kaiser, *Phys. Rev. Lett.* **89**, 163901 (2002).
- [26] C. Cohen-Tannoudji, J. Dupont-Roc, and G. Grynberg, *Photons and Atoms: Introduction to Quantum Electrodynamics* (Wiley, New York, 1992).
- [27] O. Morice, Y. Castin, and J. Dalibard, *Phys. Rev. A* **51**, 3896 (1995).
- [28] Ya. A. Fofanov, A. S. Kuraptsev, I. M. Sokolov, and M. D. Havey, *Phys. Rev. A* **84**, 053811 (2011).
- [29] I. M. Sokolov, D. V. Kupriyanov, and M. D. Havey, *J. Exp. Theor. Phys.* **112**, 246 (2011).
- [30] L. Bellando, A. Gero, E. Akkermans, and R. Kaiser, *Phys. Rev. A* **90**, 063822 (2014).
- [31] F. A. Pinheiro, M. Rusek, A. Orłowski, and B. A. van Tiggelen, *Acta Phys. Pol. A* **105**, 339 (2004).
- [32] A. Goetschy and S. E. Skipetrov, *Phys. Rev. E* **84**, 011150 (2011).
- [33] S. E. Skipetrov and A. Goetschy, *J. Phys. A* **44**, 065102 (2011).
- [34] S. Balik, A. L. Win, M. D. Havey, I. M. Sokolov, and D. V. Kupriyanov, *Phys. Rev. A* **87**, 053817 (2013).
- [35] J. Pellegrino, R. Bourgain, S. Jennewein, Y. R. P. Sortais, A. Browaeys, S. D. Jenkins, and J. Ruostekoski, *Phys. Rev. Lett.* **113**, 133602 (2014).
- [36] J. Wang and A. Z. Genack, *Nature (London)* **471**, 345 (2011).
- [37] M. Gross and S. Haroche, *Phys. Rep.* **93**, 301 (1982).
- [38] See Supplemental Material at <http://link.aps.org/supplemental/10.1103/PhysRevLett.114.053902>, which includes Refs. [39–45], for additional evidence of the localization transition.
- [39] F. A. Pinheiro, M. Rusek, A. Orłowski, and B. A. van Tiggelen, *Phys. Rev. E* **69**, 026605 (2004).
- [40] E. Akkermans, A. Gero, and R. Kaiser, *Phys. Rev. Lett.* **101**, 103602 (2008).
- [41] T. Kottos, *J. Phys. A* **38**, 10761 (2005).
- [42] A. Goetschy, Ph.D. thesis, J. Fourier Univ., Grenoble, 2011.
- [43] M. L. Mehta, *Random Matrices* (Elesvier, Amsterdam, 2004).
- [44] F. Haake, *Quantum Signatures of Chaos* (Springer-Verlag, Berlin, 2001).
- [45] D. A. Varshalovich, A. N. Maskalev, and V. K. Khersonskii, *Quantum Theory of Angular Momentum* (World Scientific, Singapore, 1988).
- [46] Y. Bidel, B. Klappauf, J. C. Bernard, D. Delande, G. Labeyrie, C. Miniatura, D. Wilkowski, and R. Kaiser, *Phys. Rev. Lett.* **88**, 203902 (2002).
- [47] A. S. Sheremet, A. D. Manukhova, N. V. Larionov, and D. V. Kupriyanov, *Phys. Rev. A* **86**, 043414 (2012).